

Research Article

Open Access, Volume 6

MRI-Guided Percutaneous Cryoablation of Hepatic Tumors in Pericardiac Locations: A Case Series

Setayesh Sotoudehnia Korani; Aiming Lu; Ola AE Mohamed; Scott M Thompson; Daniel Adamo; David A Woodrum*

Department of Radiology, Mayo Clinic, Rochester, MN, USA.

Abstract

Background: Percutaneous ablation of hepatic tumors in pericardiac locations poses a recognized technical challenge due to limited acoustic windows, proximity to the myocardium and phrenic nerve, and risk of non-target thermal injury. MRI guidance offers superior soft-tissue contrast and real-time ice ball visualization, potentially enabling safer treatment of such lesions. We report our institutional experience with MRI-guided cryoablation of pericardiac hepatic tumors.

Methods: Five patients (4 men, 1 woman; mean age 65.6 ± 11.5 years) with six pericardiac or subdiaphragmatic hepatic lesions underwent MRI-guided percutaneous cryoablation. Lesion-to-cardiac structure distance ranged from 3.2 to 7.5 mm. Primary endpoints were technical success and absence of cardiac complications. Local tumor control and follow-up duration were secondary endpoints.

Results: All procedures were technically successful (100%). No cardiac, pericardial, or phrenic nerve complications occurred. At median follow-up of 27 months (range 19-44), no patient developed in-field local tumor progression. One patient (Patient 3) developed out-of-field hepatic progression at 27 months, unrelated to the treated pericardiac lesion.

Conclusion: MRI-guided cryoablation of pericardiac hepatic tumors is feasible and safe, with 100% technical success and no cardiac complications at a median follow-up of 27 months. Real-time MRI ice ball monitoring enables precise margin control in proximity to the heart without collateral injury.

Keywords: Cryoablation; Liver neoplasms; Magnetic resonance imaging; Pericardiac; Image-guided ablation; Interventional radiology.

Introduction

The liver is one of the most frequent sites of both primary and metastatic malignancy. Percutaneous image-guided ablation has emerged as a critical treatment option for patients with oligometastatic or primary hepatic disease who are not surgical candidates, offering local tumor control with low morbidity and preservation of functional hepatic parenchyma [1,2]. Cryoablation, induces tumor cell death through repetitive freeze-thaw cycles causing intracellular ice crystal formation, membrane disruption,

and ischemic necrosis. This technique offers procedural advantages over heat-based modalities, including direct visualization of the ablation zone as an ice ball and a favorable safety profile near vulnerable structures [3,4].

Hepatic lesions in pericardiac locations - the hepatic dome, subdiaphragmatic segments (particularly segments II, IV, and VIII), and regions immediately adjacent to the right atrium - represent a particularly challenging subset for percutaneous ablation. These lesions are difficult to access under ultrasound or CT guidance

Manuscript Information: Received: May 16, 2026; Accepted: Jun 01, 2026; Published: Jun 08, 2026

Correspondance: David A Woodrum, Department of Radiology, Mayo Clinic, Rochester, MN, USA.

Email: woodrum.david@mayo.edu

Citation: Korani SS, Lu A, Mohamed OAE, Thompson SM, Woodrum DA, et al. MRI-Guided Percutaneous Cryoablation of Hepatic Tumors in Pericardiac Locations: A Case Series. *J Oncology*. 2026; 6(1): 1206.

Copyright: © Woodrum DA 2026. Content published in the journal follows creative common attribution license.

due to rib shadowing and limited acoustic windows, and carry the theoretical risk of thermal injury to the myocardium, pericardium, and phrenic nerve [5,6]. Consequently, such lesions are frequently considered inoperable or technically prohibitive by conventional ablation criteria.

Beyond imaging limitations, heat-based modalities carry an inherent cardiac risk at pericardiac locations: experimental data have demonstrated that microwave ablation within 5 mm of the pericardium is associated with cardiac arrhythmias and direct myocardial thermal injury through heat propagation to adjacent autonomic and myocardial tissue, and a clinical case of late hemorrhagic pericarditis with cardiac tamponade following hepatic MWA of a Segment II lesion near the diaphragm has been reported [7,8]. Cardiac tamponade is a recognized though rare complication of hepatic RFA for dome and left-lobe lesions, with multiple fatal cases reported in the literature involving tumors in segments II and IV adjacent to the diaphragm [9,10]. These risks are not shared by cryoablation, where the ablation zone is physically bounded by the ice ball and myocardial injury requires direct contact rather than thermal propagation.

Magnetic Resonance Imaging (MRI) offers unique advantages for guiding ablation in these locations. Superior soft-tissue contrast allows precise tumor delineation, while the hypointense ice ball on T2-weighted sequences enables real-time, multiplanar monitoring of ablation margin relative to adjacent cardiac structures - a capability not reliably available with CT or ultrasound guidance [11-13]. Despite these theoretical benefits, published data specifically addressing the safety and feasibility of MRI-guided cryoablation in pericardiac hepatic locations remain limited.

We report a single-center case series of five patients with hepatic tumors in pericardiac locations who underwent MRI-guided percutaneous cryoablation, with particular emphasis on cardiac safety, technical approach, and local tumor control at long-term follow-up.

Materials and methods

Study design and patient selection: This retrospective single-center case series was conducted with institutional review board approval and a waiver of informed consent. From a prospectively maintained database of all patients undergoing MRI-guided percutaneous cryoablation for hepatic tumors at our institution between January 2019 and January 2025, we identified five patients with lesions in pericardiac or subdiaphragmatic hepatic locations (lesion-to-cardiac structure distance ≤ 10 mm on pre-procedural MRI) who had more than a year follow up. Patient and procedural characteristics are summarized in (Table 1).

MRI-guided cryoablation technique: All procedures were performed in a 1.5T MRI suite under general anesthesia. Initial needle access was achieved with real-time ultrasound guidance using an Abacate introducer. One to five 17-gauge Ice Rod cry needles (Boston Scientific Visual ICE, Marlborough, MA) were advanced to the target lesion under intermittent MRI confirmation.

Ablation was performed with three to four freeze-thaw cycles. T2-weighted MRI sequences were acquired continuously during freezing to monitor ice ball formation and ensure complete tumor

coverage with an adequate margin, with particular attention to the relationship of the ice ball margin to the cardiac silhouette and diaphragm. The goal was to maintain a visible T2 signal interface between the ice ball and cardiac structures, precluding direct contact. After the final thaw cycle, cry needles were withdrawn and Gel foam slurry was injected through the introducer sheath for hemostasis.

Follow-up and outcome assessment: Post-procedural follow-up was performed with contrast-enhanced MRI or CT/PET at 3, 6, 9, and 12 months, and annually thereafter. Primary endpoints were technical success (satisfactory needle placement and completion of planned freeze-thaw cycles with ice ball coverage of the target lesion) and absence of cardiac, pericardial, or phrenic nerve complications. Secondary endpoints included in-field local tumor control (absence of residual or recurrent enhancement within or at the margin of the ablation zone) and overall follow-up duration without in-field progression.

Results

Patient and procedural characteristics: Five patients (4 men, 1 woman; mean age 65.6 ± 11.5 years; range 56-85) underwent MRI-guided cryoablation of six pericardiac or subdiaphragmatic hepatic lesions across five sessions. Tumor histology included prostate cancer metastases (n=2), colorectal/rectal cancer metastases (n=2), and cholangiocarcinoma (n=1). Mean lesion size was 15.4 ± 4.8 mm (range 10-20 mm). Mean icefall-to-cardiac structure distance was 5.0 ± 1.7 mm (range 3.2-7.5 mm). The number of cry needles per session ranged from 1 to 5 (Table 1). Three to four freeze-thaw cycles were performed per session.

Technical success and cardiac safety: All five procedures (100%) were technically successful. Post-ablation MRI in all cases demonstrated ice ball coverage of the target lesion with preservation of a visible T2 signal interface between the ablation margin and the cardiac silhouette. No cardiac arrhythmia, pericardial effusion, phrenic nerve palsy, or other cardiac complications occurred in any patient during the procedure or within the periprocedural period. No patient required overnight observation for cardiac monitoring beyond standard post-procedural protocol.

Local tumor control and follow-up: At a median follow-up of 27 months (range 19-44 months), no patient developed in-field local tumor progression at the treated pericardiac lesion. Technique efficacy (absence of residual enhancement at the ablation zone on 3-month imaging) was confirmed in all cases. One patient (Patient 3, prostate metastases) developed out-of-field hepatic progression at 27 months; this represented new lesions beyond the ablation zone and did not constitute local control failure of the pericardiac lesion. Patient 5 (colorectal metastasis, 3.2 mm from pericardium) demonstrated the closest cardiac proximity and longest recurrence-free follow-up at 44 months.

Representative MRI and PET/CT imaging for all five patients, demonstrating pre-procedural lesion-to-cardiac proximity, intraprocedural ice ball formation with preserved pericardiac T2 signal, and follow-up confirmation of local tumor control, are presented in (Figures 1-5).

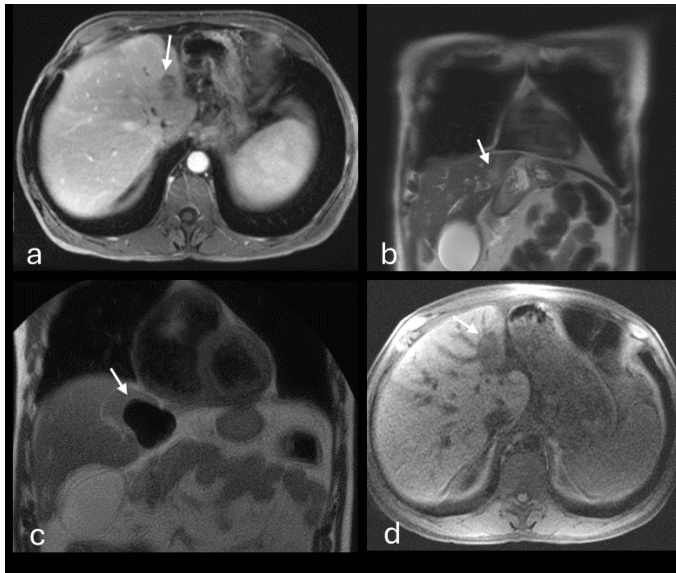


Figure 1: 59-year-old male with cholangiocarcinoma metastasis in hepatic segment II, 7.5 mm from the cardiac silhouette. **(a)** Pre-procedural axial contrast-enhanced T1-weighted MRI demonstrating the index lesion (arrow) in the left hepatic lobe adjacent to the diaphragm. **(b)** Coronal T2-weighted MRI showing the lesion (arrow) in relation to the overlying cardiac border. **(c)** Intraprocedural coronal T2-weighted MRI demonstrating the hypointense iceball (arrow) with preserved T2 signal between the ablation zone and the myocardium. **(d)** Follow-up axial contrast-enhanced T1-weighted MRI showing a non-enhancing ablation zone (arrow) without local tumor progression.

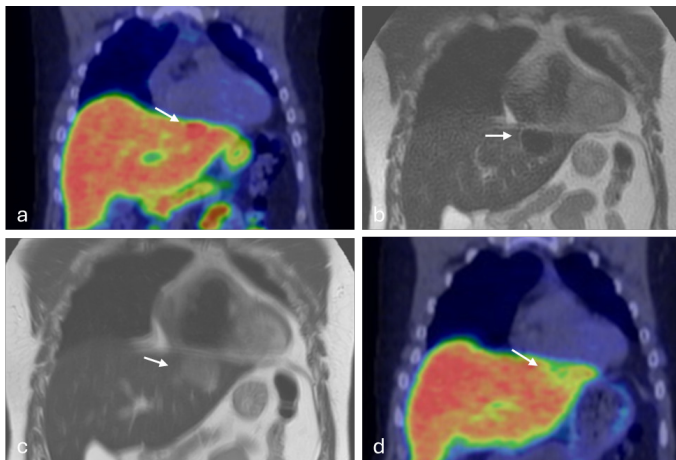


Figure 2: 85-year-old male with prostate cancer metastasis in the subdiaphragmatic left hepatic lobe, 5 mm from the cardiac silhouette. **(a)** Pre-procedural coronal PET/CT demonstrating an FDG-avid lesion (arrow) inferior to the cardiac border. **(b)** Coronal T2-weighted MRI showing the lesion (arrow) immediately beneath the diaphragm. **(c)** Immediate post-ablation axial T2-weighted MRI demonstrating the signal-void iceball (arrow) with a preserved T2 interface between the ablation zone. **(d)** Follow-up coronal PET/CT demonstrating complete metabolic response (arrow) with no in-field local tumor progression.

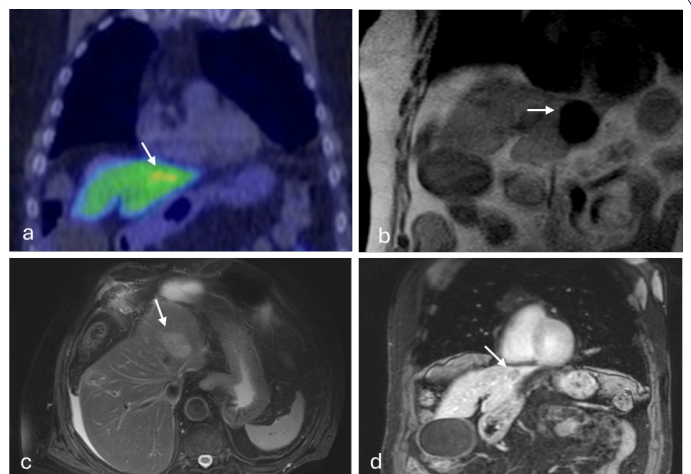


Figure 3: 56-year-old male with prostate cancer metastasis in hepatic segment II abutting the diaphragm, 3.2 mm from the cardiac structure. **(a)** Pre-procedural coronal PET/CT demonstrating FDG-avid activity (arrow) at the hepatic dome immediately inferior to the cardiac border. **(b)** Pre-procedural coronal contrast-enhanced T1-weighted MRI showing the enhancing lesion (arrow) abutting the diaphragm. **(c)** Immediate post-ablation coronal T2-weighted MRI demonstrating the hypointense iceball (arrow) at the hepatic dome with preserved T2 signal at the superior margin, confirming absence of myocardial contact. **(d)** Follow-up coronal PET/CT demonstrating complete metabolic response (arrow) with no in-field local tumor progression.

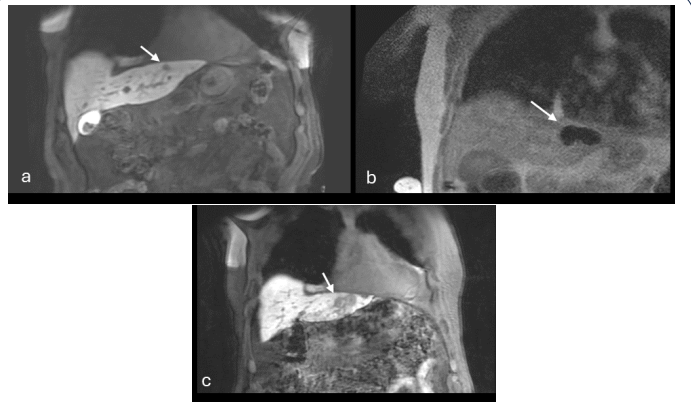


Figure 4: 71-year-old male with rectal cancer metastasis in the right hepatic lobe, 6 mm from the cardiac structure. **(a)** Pre-procedural coronal contrast-enhanced T1-weighted MRI demonstrating the enhancing lesion (arrow) in the right lobe with the cardiac silhouette visible superiorly. **(b)** Intraprocedural coronal T2-weighted MRI demonstrating the hypointense iceball (arrow) with preserved T2 signal between the ablation zone and the cardiac border. **(c)** Follow-up coronal contrast-enhanced T1-weighted MRI demonstrating a non-enhancing ablation zone (arrow) without residual tumor; no in-field progression.

Table 1: Patient and procedural characteristics.

Pt	Cancer Type	Sex/Age	Location	Size (mm)	Dist. to Heart (mm)	Needles	Cycles	Follow-up (MO)	Local Recurrence
1	Cholangiocarcinoma	M/59	Left lobe (Seg II)	18	7.5	2	3	19	None
2	Prostate metastasis	M/85	Left lobe	11	5	2	3	31	None
3	Prostate metastasis	M/56	Seg II immediately abutting diaphragm	20	3.2	2	3	27	None
4	Rectal cancer metastasis	M/71	left lobe	18	6	2	4	22	None
5	Colorectal metastasis	F/57	Anterior hepatic dome	10	3.2	2	3	44	None

Pt: Patient; Dist.: Distance to cardiac structure on pre-procedural MRI.

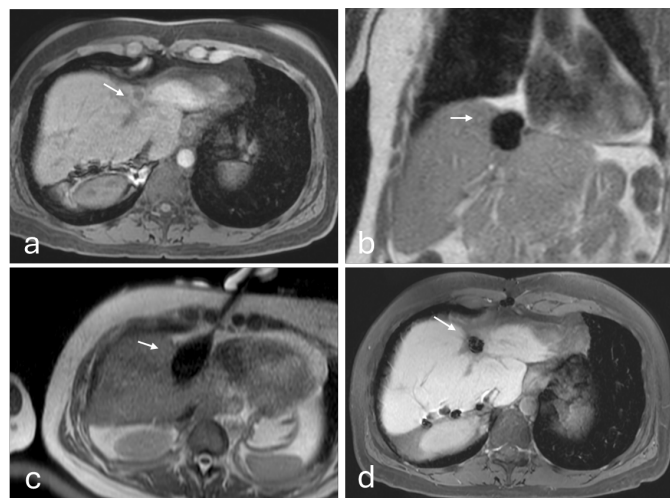


Figure 5: 57-year-old female with colorectal cancer metastasis at the anterior hepatic dome, 3.2 mm from the pericardium - the closest cardiac proximity in this series. **(a)** Pre-procedural axial contrast-enhanced T1-weighted MRI demonstrating the 10-mm enhancing lesion at the anterior dome. **(b)** Coronal T2-weighted MRI confirming the 3.2 mm lesion-to-pericardium distance. **(c)** Intraprocedural axial T2-weighted MRI during active cryoablation demonstrating cryoneedle placement (arrow) and iceball formation at the dome; preserved T2 signal between the iceball periphery and the pericardial reflection confirms absence of myocardial contact at the closest proximity in this series. **(d)** Follow-up axial T2-weighted MRI demonstrating a hypointense ablation scar without local tumor progression.

Discussion

This case series demonstrates that MRI-guided percutaneous cryoablation of pericardiac hepatic tumors is technically feasible and safe, with 100% technical success and no cardiac complications across five procedures at ice ball-to-cardiac distances as close as 3.2 mm. At a median follow-up of 27 months, all treated pericardiac lesions remained free of in-field local tumor progression, supporting the durability of the technique in this anatomically challenging location.

Pericardiac and subdiaphragmatic hepatic lesions - those in segments II, IV, VII, and VIII abutting the diaphragm, right atrium, or inferior vena cava - are frequently excluded from percutaneous ablation series or classified as high-risk due to limited needle access and proximity to cardiac structures [5,6]. Thermal injury

to the myocardium is a recognized theoretical risk of both heat-based and cryo-based ablation in these locations. Microwave Ablation (MWA) at pericardiac hepatic locations carries distinct risks not present with cryoablation. Experimental porcine models have demonstrated that MWA within 5 mm of the pericardium is associated with a significantly increased risk of cardiac arrhythmias and direct thermal myocardial injury, with arrhythmias arising not from electromagnetic interference per se but from heat-mediated depolarization of adjacent myocardial or autonomic nerve tissue [7,14]. Clinically, a case of late hemorrhagic pericarditis and cardiac tamponade has been reported following hepatic MWA for a Segment II metastasis near the diaphragm, highlighting the potential severity of thermal injury in this anatomic zone [8]. Cryoablation carries no analogous electromagnetic or thermal propagation risk; myocardial injury is only possible through direct ice ball contact, which real-time T2-weighted MRI monitoring is specifically designed to prevent.

Cryoablation offers a potential advantage in this context: the ice ball is sharply demarcated as a T2 signal void on MRI, enabling real-time assessment of the margin between the frozen zone and the cardiac wall [12,13]. This allows the operator to confirm that the ablation zone encompasses the tumor while avoiding direct contact with the myocardium - a level of margin control not reliably available with CT guidance, where the ice ball edge may be indistinct, or with ultrasound, where cardiac shadow may obscure the critical interface.

The mean ice ball-to-cardiac distance in our series (5.0 mm) is notably smaller than published series describing ablation of «difficult location» hepatic tumors, which typically define proximity as within 1 cm of major vascular structures rather than the cardiac silhouette specifically [15]. The closest proximity in our series (3.2 mm, Patient 5) is, to our knowledge, among the smallest reported margins from the pericardium for percutaneous hepatic cryoablation without cardiac complication. The long recurrence-free follow-up of 44 months in this patient further supports the adequacy of the ablative margin despite extreme cardiac proximity.

The use of combined US/MR guidance was instrumental in achieving accurate needle placement for subdiaphragmatic lesions not well-visualized by ultrasound alone. MR fluoroscopy - in this context, rapid near-continuous T2 acquisition updated approximately every 20 seconds - provided real-time ice ball boundary monitoring throughout the freeze cycles, consistent with established workflows for interventional MRI [13,16].

Limitations of this case series include its small sample size (n=5), retrospective design, heterogeneous tumor histology, and absence of a comparator group treated by alternative guidance modalities. The series does not permit conclusions about comparative efficacy versus CT-guided cryoablation or heat-based ablation at pericardiac locations. Nevertheless, these cases represent a concentrated subset of the highest-risk hepatic ablation scenarios, and the absence of any cardiac complication across all five procedures provides meaningful safety data for an underreported topic.

Conclusion

MRI-guided percutaneous cryoablation of pericardiac hepatic tumors is feasible and safe. Real-time T2-weighted MRI monitoring of ice ball expansion enables precise ablative margin control at cardiac proximity as close as 3.2 mm without cardiac complication. Local tumor control was maintained in all five patients at a median follow-up of 27 months, supporting the oncologic efficacy of this approach at anatomically challenging locations. MRI guidance should be considered the modality of choice when percutaneous ablation is undertaken for hepatic lesions in pericardiac or subdiaphragmatic positions.

References

1. Lencioni R, de Baere T, Martin RC, Nutting CW, Narayanan G. Image-guided ablation of malignant liver tumors: Recommendations for clinical validation of novel thermal and non-thermal technologies. *Liver Cancer*. 2015; 4(4): 208-214.
2. Kolck J, et al. Percutaneous cryoablation in the liver: A meta-analysis. *Cardiovasc Intervent Radial*. 2024. doi:10.1007/s00270-024-03869-9.
3. Gage AA, Baust J. Mechanisms of tissue injury in cryosurgery. *Cryobiology*. 1998; 37(3): 171-186.
4. Glazer DI, Tatli S, Shyn PB, Silverman SG. Percutaneous image-guided cryoablation of hepatic tumors: intermediate to long-term outcomes. *AJR Am J Roentgenol*. 2017; 209(4): 205-213.
5. Littrup PJ, Aoun HD, Adam B, et al. Percutaneous cryoablation of hepatic tumors: Long-Term experience of a large U.S. series. *Abdom Radial (NY)*. 2016; 41(4): 767-780.
6. Pusceddu C, Melis L, Ballicu N, et al. Cryoablation of liver lesions: Clinical data, complications, and review of the literature. *J Gastrointest Cancer*. 2022; 53(3): 765-773.
7. Carberry GA, Nocerino E, Mason PJ, Schwahn DJ, Hetzel S, et al. Pulmonary microwave ablation near the heart: antenna positioning can mitigate cardiac complications in a porcine model. *Radiology*. 2017; 282(3): 892-902.
8. Pavon AG, Rubimbura V, Nowacka A, Hocquelet A, Schwitter J, et al. Case report: Acute pericarditis following hepatic microwave ablation for liver metastasis. *Front Cardiovasc Med*. 2023; 10: 1100916.
9. Moumouh A, Hannequin J, Chagneau C, Rayeh F, Jeanny A, et al. A tamponade leading to death after radiofrequency ablation of hepatocellular carcinoma. *Eur Radiol*. 2005; 15(2): 234-237. doi:10.1007/s00330-004-2485-z. PMID: 15503044. PubMed
10. Gao J, Sun WB, Tong ZC, Ding XM, Ke S. Successful treatment of acute hemorrhagic cardiac tamponade in a patient with hepatocellular carcinoma during percutaneous radiofrequency ablation. *Chin Med J (Engl)*. 2010; 123(11): 1470-1472. PMID available via PubMed.
11. Gangi A, Tsoumakidou G, Abdelli O, et al. MR-guided percutaneous interventions: An overview. *Semin Intervent Radiol*. 2012; 29(3): 195-202.
12. Silverman SG, Tuncali K, Adams DF, et al. MR imaging-guided percutaneous cryotherapy of liver tumors: Initial experience. *Radiology*. 2000; 217(3): 657-664.
13. Thompson SM, Gorny KR, Koepsel EMK, et al. Body interventional MRI for diagnostic and interventional radiologists: current practice and future prospects. *Radiographic*. 2021; 41(6): 1785-1801.
14. Hinshaw JL, Lubner MG, Ziemlewicz TJ, Lee FT Jr, Brace CL. Percutaneous tumor ablation tools: Microwave, radiofrequency, or cryoablation - what should you use and why? *Radiographic*. 2014; 34(5): 1344-1362.
15. Shyn PB, Tatli S, Sahni VA, et al. Percutaneous imaging-guided cryoablation of liver tumors: predicting local progression on early post-ablation MRI. *AJR Am J Roentgenol*. 2014; 203(2): 181-191.
16. Woodrum DA, Kawashima A, Gorny KR, Mynderse LA. MR imaging-guided cryoablation. *Magna Reason Imaging Clin N Am*. 2012; 20(2): 253-264.